

Eliminating frequency and space-time correlations in multiphoton states

W. P. Grice

Center for Engineering Science Advanced Research, Computer Science and Mathematics Division, Oak Ridge National Laboratory, Oak Ridge, Tennessee 37831

A. B. U'Ren and I. A. Walmsley

The Institute of Optics, University of Rochester, Rochester, New York 14627

(Received 27 March 2001; published 19 November 2001)

Multiphoton states constructed from photon pairs generated in the process of spontaneous parametric down-conversion possess frequency and space-time correlations that may carry undesired distinguishing information. It is shown that these correlations may be eliminated if certain conditions in the source configuration are satisfied. For the cases in which these conditions cannot be satisfied because of experimental constraints, it is shown that the correlations may be reduced through proper choices of crystal length and pump bandwidth. The advantage of such source engineering is that it yields much higher count rates, since no photon pairs are lost by predetection spectral filtering.

DOI: 10.1103/PhysRevA.64.063815

PACS number(s): 42.50.Dv, 03.65.Ud, 42.65.Ky

Entangled pairs of photons play a central role in fundamental tests of quantum mechanics, as well as in several quantum communications technologies. The recent demonstrations of quantum teleportation [1], entanglement swapping [2], and three-photon entanglement [3,4] all rely on this resource for their success. In all these cases, the photons were entangled with respect to their polarization degree of freedom. Care must be taken, however, in appropriately engineering the other degrees of freedom (the directions of travel, arrival times, or wavelengths) if either entanglement or the availability of distinguishing information in these degrees of freedom may compromise the interference procedures central to experiments of this kind. Both teleportation and entanglement swapping rely on Bell-state measurement and in these, it was essential that some or all of the photons were detected in such a way that it was impossible to determine their origins. When experiments involve the interference of photons from different sources, it turns out that this may be quite difficult, since strong frequency or space-time correlations often exist between *pairs* of photons comprising the multiphoton state.

The problem of distinguishing information is most pressing when photon pairs are generated using spontaneous parametric fluorescence. Currently, this method is the most promising for the generation of a multiphoton state since it minimizes, in practical terms, the number of sources required to generate the multiphoton state [5,6]. It is possible to generate an even-numbered photon multiplet by concatenating several biphoton sources, each of which is pumped by a short optical pulse whose duration is less than the coherence time of the emitted photon wave packet. In this case, the photons are emitted spontaneously, but the times of emission are known to within the duration of the pump pulse. This eliminates most, but not all, of the distinguishing timing information [7] (a small amount of temporal information remains due to the different group velocities experienced by the pump field and the signal and idler fields). Information associated with the energies of the photons is more difficult to eliminate, however, as there is typically a strong correlation

between the frequencies of the signal and idler photons. Because of these correlations, it is occasionally possible to identify pairs of photons as siblings. By measuring the frequencies of the photons detected in a multisource experiment, one could determine, with some degree of certainty, the source of a pair of photons. Unfortunately, this is enough information to seriously degrade fidelity of the inference that the input photons were in, say, the Bell-polarization singlet state.

The challenge in an experiment involving three or more photons may be summed up as follows: the experimentalist wishing to take advantage of the simultaneous generation of two photons in a down-conversion event must find some way to negate the deleterious effects of their strong frequency correlations. One approach to this problem is to eliminate the frequency entanglement by filtering the ensemble of photon pairs just prior to detection, retaining only those lacking distinguishing information. With the sources employed to date, this may be accomplished only if the spectral filters are quite narrow, thus resulting in a prohibitively low-count rate [6]. This appears to be the greatest stumbling block to the development of viable multiphoton sources, since the rate at which two or three crystals will emit photons simultaneously is quite low, even without filtering.

In this paper, we propose a more direct solution to this problem. It is shown that, by adjusting parameters such as crystal length, crystal material, and the bandwidth and center wavelength of the pump, it is possible to configure a down-conversion crystal in which the signal and idler are *completely uncorrelated* in frequency. With this type of source, it is not necessary to take steps to eliminate distinguishing spectral information since no such information exists. Unlike the method described above, therefore, every photon pair may be used and none need be discarded. We show, furthermore, that the photons emitted from such sources are also free of space-time correlations. Finally, we show that steps may be taken to minimize frequency correlations, even when experimental constraints do not permit them to be eliminated entirely.

If the frequencies of the photons emitted from a down-conversion source are truly uncorrelated, then the frequency of either of the photons should yield absolutely no information about the frequency of its conjugate. This condition is satisfied if the signal and idler frequencies are statistically independent. That is,

$$S(\omega_s, \omega_i) = p_s(\omega_s)p_i(\omega_i), \quad (1)$$

where $p_s(\omega_s)$ [$p_i(\omega_i)$] is the probability that the signal [idler] photon has frequency ω_s [ω_i] and the joint spectral intensity $S(\omega_s, \omega_i)$ is the probability that the signal photon has frequency ω_s and the idler photon has frequency ω_i . We note that this condition is not satisfied in any biphoton source demonstrated to date. Because they are related to the pump frequency, there is often a strong correlation between the signal and idler frequencies.

To calculate $S(\omega_s, \omega_i)$, it is useful to imagine a pair of energy-sensitive detectors monitoring the signal and idler beams. The joint spectral intensity is simply the probability that a photon of frequency ω_s is detected in the signal beam and a photon of frequency ω_i is detected in the idler beam. For a two-photon state given by

$$|\psi\rangle = \frac{1}{(2\pi)^2} \int \int d\omega_s d\omega_i f(\omega_s, \omega_i) \hat{a}_s^\dagger(\omega_s) \hat{a}_i^\dagger(\omega_i) |\text{vac}\rangle, \quad (2)$$

where $\hat{a}_s^\dagger(\omega_s)$ and $\hat{a}_i^\dagger(\omega_i)$ are the photon creation operators for the signal and idler beams, the joint spectral intensity is

$$\begin{aligned} S(\omega_s, \omega_i) &= \langle \psi | \hat{a}_s^\dagger(\omega_s) \hat{a}_i^\dagger(\omega_i) \hat{a}_s(\omega_s) \hat{a}_i(\omega_i) | \psi \rangle \\ &= |f(\omega_s, \omega_i)|^2. \end{aligned} \quad (3)$$

It is seen by comparing this equation to Eq. (1) that the signal and idler frequencies are independent only if $f(\omega_s, \omega_i)$ can be factored, that is only if there exist some $f_s(\omega_s)$ and $f_i(\omega_i)$ such that $f(\omega_s, \omega_i) = f_s(\omega_s)f_i(\omega_i)$. It is worth noting that if $f(\omega_s, \omega_i)$ may be factored in this way, then the two-photon state $|\psi\rangle$ is not entangled in frequency, since it may be written as

$$\begin{aligned} |\psi\rangle &= \frac{1}{(2\pi)^2} \int \int d\omega_s d\omega_i f_s(\omega_s) f_i(\omega_i) \hat{a}_s^\dagger(\omega_s) \hat{a}_i^\dagger(\omega_i) |\text{vac}\rangle \\ &= \left[\frac{1}{2\pi} \int d\omega_s f_s(\omega_s) \hat{a}_s^\dagger(\omega_s) \right] \\ &\quad \times \left[\frac{1}{2\pi} \int d\omega_i f_i(\omega_i) \hat{a}_i^\dagger(\omega_i) \right] |\text{vac}\rangle, \end{aligned} \quad (4)$$

which is a direct product state.

In addition to having no frequency correlation, this type of two-photon state is also free of space-time correlation. That is, the probability distribution for the time of detection of a signal photon, for example, is independent of the idler detection time. To show that this is the case, we calculate the joint temporal intensity, which is given by

$$I(t_s, t_i) = \langle \hat{a}_s^\dagger(t_s) \hat{a}_i^\dagger(t_i) \hat{a}_s(t_s) \hat{a}_i(t_i) \rangle, \quad (5)$$

where

$$\hat{a}_\mu(t) = \frac{1}{2\pi} \int d\omega \hat{a}_\mu(\omega) e^{-i\omega t} \quad (\mu = s, i). \quad (6)$$

It is not difficult to show that if the joint spectral intensity is given by $S(\omega_s, \omega_i) = |f_s(\omega_s)f_i(\omega_i)|^2$, then the joint temporal intensity is

$$I(t_s, t_i) = |g_s(t_s)g_i(t_i)|^2, \quad (7)$$

where

$$g_\mu(t) = \frac{1}{2\pi} \int d\omega f_\mu(\omega) e^{-i\omega t} \quad (\mu = s, i). \quad (8)$$

Thus, if the frequencies of the signal and idler photons are uncorrelated, then so are their emission times. That is not to say that the photons are emitted at random times. On the contrary, each is emitted within a time interval whose duration is on the order of the pump-pulse duration. Beyond that constraint, however, the emission time of one photon is completely independent of the emission time of its conjugate.

Returning to the frequency domain, the general expression for the probability amplitude of the two-photon state generated in the process of spontaneous parametric down-conversion is [8]

$$f(\omega_s, \omega_i) = N\alpha(\omega_s + \omega_i)\phi(\omega_s, \omega_i), \quad (9)$$

where N is a normalization constant, $\alpha(\omega_s + \omega_i)$ is a function describing the envelope of the pump field, and $\phi(\omega_s, \omega_i)$ is a phase-matching function given by

$$\begin{aligned} \phi(\omega_s, \omega_i) &= \text{sinc} \left\{ \frac{L}{2} [k_p(\omega_s + \omega_i) - k_s(\omega_s) - k_i(\omega_i)] \right\} \\ &\quad \times \exp \left\{ -i \frac{L}{2} [k_p(\omega_s + \omega_i) - k_s(\omega_s) - k_i(\omega_i)] \right\}. \end{aligned} \quad (10)$$

In this expression, $k_p(\omega)$ [$k_s(\omega)$, $k_i(\omega)$] is the wave number for the pump [signal, idler] beam and L is the crystal length. A plot of $S(\omega_s, \omega_i) = |\alpha(\omega_s + \omega_i)\phi(\omega_s, \omega_i)|^2$ for a type-II beta-barium borate (BBO) crystal oriented for collinear down-conversion of a pump field with a center wavelength of 400 nm is shown in Fig. 1 (the treatment for the noncollinear case is similar). The plot indicates that the depicted state is not maximally correlated in frequency, since there is not a strict one-to-one relationship between the signal and idler frequencies. Rather, detection of a particular idler frequency specifies a range of frequencies available for the signal photon. On the other hand, the correlation is not zero, since the range of signal frequencies depends on the particular idler frequency detected. The correlation could be reduced or eliminated if it were somehow possible to "rotate" this joint spectral intensity so that its major axis were parallel to one of the two frequency axes.

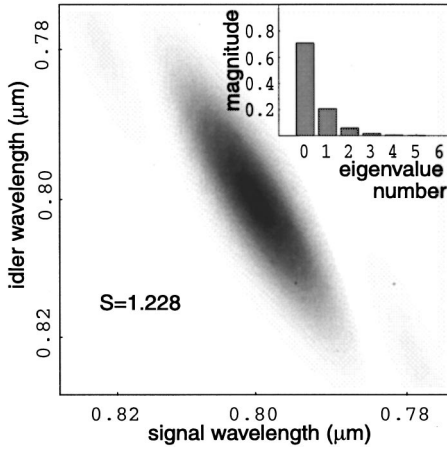


FIG. 1. The joint spectral intensity for degenerate type-II down-conversion in BBO with a 400 nm pump. In this and subsequent figures, the two axes represent the signal and idler frequencies, although as an aid to the reader, the frequencies have been converted to wavelength. The inset shows the numerical value of the entropy of entanglement, as well as the magnitudes of the first seven eigenvalues in the Schmidt decomposition of the two-photon state.

The shape of $S(\omega_s, \omega_i)$ depends, of course, on the shapes of the functions $|\alpha(\omega_s + \omega_i)|^2$ and $|\phi(\omega_s, \omega_i)|^2$. To understand this relationship, it is instructive to examine plots of these functions individually. The pump envelope function shown in Fig. 2(a) is assumed to have a Gaussian shape with a width that is proportional to the spectral width of the pump field. Since the argument of $|\alpha(\omega_s + \omega_i)|^2$ is the sum of the frequencies ω_s and ω_i , the function has constant value along lines defined by $\omega_s + \omega_i = \text{const}$ and reaches its peak value at every point on the line

$$\omega_s + \omega_i = \bar{\omega}_s + \bar{\omega}_i = \bar{\omega}_p, \quad (11)$$

where $\bar{\omega}_s$, $\bar{\omega}_i$, and $\bar{\omega}_p$ are the center frequencies of the signal, idler, and pump fields, respectively.

Figure 2(b) shows a plot of $|\phi(\omega_s, \omega_i)|^2$, which has a somewhat more complicated shape in the signal-idler frequency space. It may be thought of as a ridge lying along the contour defined by setting the argument of the sinc function to zero, i.e., $0 = k_p(\omega_s + \omega_i) - k_s(\omega_s) - k_i(\omega_i)$. By retaining only the lowest-order terms in power expansions about the center frequencies, and assuming perfect phase matching at the center frequencies, this contour may be approximated in the overlap region as the line defined by

$$0 = (\omega_s - \bar{\omega}_s)(k'_p - k'_s) + (\omega_i - \bar{\omega}_i)(k'_p - k'_i), \quad (12)$$

where

$$k'_\mu = \left. \frac{dk_\mu(\omega)}{d\omega} \right|_{\omega = \bar{\omega}_\mu} \quad (\mu = p, s, i). \quad (13)$$

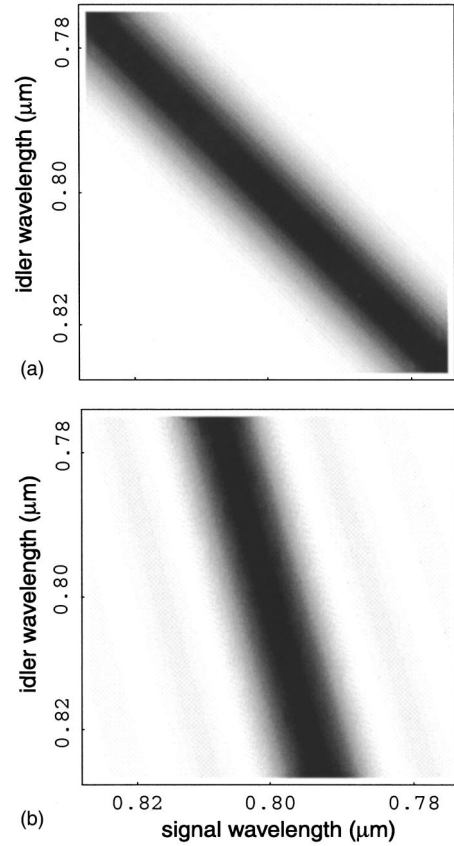


FIG. 2. The joint spectral intensity in Fig. 1 is the product of (a) the pump envelope function and (b) the phase-matching function.

In directions transverse to this contour, $|\phi(\omega_s, \omega_i)|^2$ has the shape of the square of a sinc function whose width varies inversely with the crystal length L .

The experimentalist controls the shape of the joint spectral intensity primarily through the adjustment of two parameters—the pump bandwidth and the length of the nonlinear crystal. These affect the widths of $|\alpha(\omega_s + \omega_i)|^2$ and $|\phi(\omega_s, \omega_i)|^2$, respectively. Reducing the pump bandwidth gives a narrower pump envelope function, resulting in a joint spectral intensity that lies closer to the pump envelope contour. [A monochromatic pump represents the limiting case and yields a joint spectral intensity lying exactly on the line $\omega_s + \omega_i = \omega_{\text{pump}}$.] Likewise, increasing the crystal length tends to align the joint spectral intensity more closely to the contour of Eq. (12). By adjusting these two parameters, it is possible to align the joint spectral intensity along any direction between the two extremes represented by Eqs. (11) and (12). In the BBO example given above, therefore, the joint spectral intensity will be oriented somewhere between the two functions shown in Fig. 2. Unfortunately, this range of orientations does not yield the desired factorability. That is, no combination of crystal length and pump bandwidth will eliminate frequency correlations between the signal and idler photons in type-II BBO with a 400 nm pump.

There are certain conditions, however, under which it is possible to eliminate frequency correlations entirely. This can be seen more easily if the phase-matching function is approximated by the Gaussian

$$\phi(\omega_s, \omega_i) \approx \exp\{-\gamma L^2[(\omega_s - \bar{\omega}_s)(k'_p - k'_s) + (\omega_i - \bar{\omega}_i)(k'_p - k'_i)]^2\} \exp\left\{-i \frac{L}{2}[k_p(\omega_s + \omega_i) - k_s(\omega_s) - k_i(\omega_i)]\right\}, \quad (14)$$

where $\gamma = 0.04822$. The value of this constant was chosen so that the functions $\text{sinc}(x/2)$ and $\exp(-\gamma x^2)$ have the same widths at half maximum. Taking the pump envelope function to have the form

$$\alpha(\omega_s + \omega_i) = \exp\left\{-\left[\frac{(\omega_s - \bar{\omega}_s) + (\omega_i - \bar{\omega}_i)}{\sigma}\right]^2\right\}, \quad (15)$$

the joint spectral intensity simplifies to

$$\begin{aligned} S(\omega_s, \omega_i) &= N^2 \exp\left\{-2\left[\frac{(\omega_s - \bar{\omega}_s) + (\omega_i - \bar{\omega}_i)}{\sigma}\right]^2 - 2\gamma L^2[(\omega_s - \bar{\omega}_s)(k'_p - k'_s) + (\omega_i - \bar{\omega}_i)(k'_p - k'_i)]^2\right\} \\ &= N^2 \exp\left\{-2(\omega_s - \bar{\omega}_s)^2\left[\frac{1}{\sigma^2} + \gamma L^2(k'_p - k'_s)^2\right]\right\} \exp\left\{-2(\omega_i - \bar{\omega}_i)^2\left[\frac{1}{\sigma^2} + \gamma L^2(k'_p - k'_i)^2\right]\right\} \\ &\quad \times \exp\left\{-4(\omega_s - \bar{\omega}_s)(\omega_i - \bar{\omega}_i)\left[\frac{1}{\sigma^2} + \gamma L^2(k'_p - k'_s)(k'_p - k'_i)\right]\right\}. \end{aligned} \quad (16)$$

Note that, as long as

$$\frac{1}{\sigma^2} = -\gamma L^2(k'_p - k'_s)(k'_p - k'_i), \quad (17)$$

(and as long as the Gaussian approximation is warranted) this function may be written in the form $S(\omega_s, \omega_i) = p_s(\omega_s)p_i(\omega_i)$. A quick examination of this result reveals that this condition may be met either when $k'_i < k'_p < k'_s$ or when $k'_s < k'_p < k'_i$. Since the derivative $dk/d\omega$ is the reciprocal of the group velocity, one of these inequalities will be satisfied whenever the group velocity of the pump lies between the group velocities of the signal and idler. It should be pointed out that this is impossible in degenerate type-I down-conversion—because the similarly polarized signal and idler photons have identical group velocities, the phase-matching function is oriented parallel to the pump envelope function. Although the analysis presented here neglects quadratic and higher-order dispersive terms, it is straightforward to show that if these terms are included the same conclusion is reached for type-I phase matching, i.e., neither of the above inequalities may be satisfied. In type-II crystals, however, the signal and idler photons are of different polarizations and in some cases it is possible to find wavelength ranges for which one of the above inequalities is satisfied.

None of the experiments recently reported in the literature make use of crystals meeting the above requirements. This should not be surprising, since it would require a material in which one of the daughter photons has a smaller group velocity than the pump, which necessarily has a shorter wavelength. One way to realize the required relationships between the group velocities, however, is to access different wavelength ranges, i.e., different center wavelengths for the pump, signal, and idler fields. For example, the group velocities in a BBO crystal oriented for degenerate collinear type-II

phase matching of an 800 nm pump are $v_i = 182.6 \text{ mm}/\mu\text{s}$, $v_s = 179.5 \text{ mm}/\mu\text{s}$, and $v_p = 181.4 \text{ mm}/\mu\text{s}$. Although detection is more difficult at 1.6 μm , there are some obvious

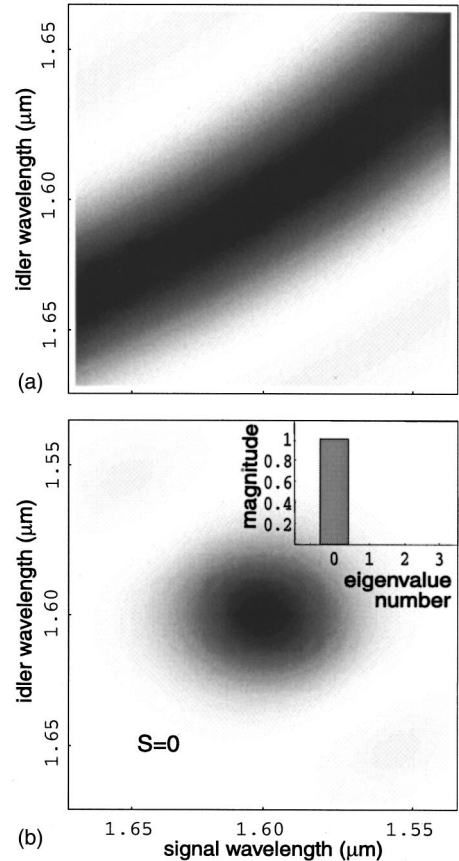


FIG. 3. (a) The phase-matching function for degenerate type-II down-conversion in BBO with an 800 nm pump. (b) The corresponding joint spectral intensity. The inset shows the details of the Schmidt decomposition.

TABLE I. Group-velocity mismatch range and group-velocity matching condition for beta-barium borate (BBO), ammonium dihydrogen phosphate (ADP), potassium dihydrogen phosphate (KDP), deuterated potassium dihydrogen phosphate (KD*P), and lithium triborate (LBO).

Material	Group-velocity mismatch range (μm)	Group-velocity matching condition (μm)
BBO	$1.169 < \lambda < 1.949$	$\lambda = 1.514$
ADP	$0.822 < \lambda < 1.637$	$\lambda = 1.082$
KDP	$0.830 < \lambda < 1.825$	$\lambda = 1.102$
KD*P	$0.952 < \lambda < 1.829$	$\lambda = 1.252$
LBO	$0.979 < \lambda < 1.771$	$\lambda = 1.283$

advantages associated with these wavelengths. The pump wavelength is easily accessed with Ti:Sapphire lasers and the $1.6 \mu\text{m}$ photons are well suited for fiber applications. Figure 3(a) shows the phase-matching function corresponding to this configuration. Recall that the orientation of the joint spectral intensity is constrained to lie somewhere between those of the phase matching and the pump envelope functions—and since the orientation of the phase-matching function is significantly different than that of the pump envelope, this configuration offers greater flexibility in crafting the shape of the joint spectral intensity.

Once a material with the proper group-velocity mismatch has been identified, the joint spectral intensity may be engineered by adjusting the relative widths of the pump envelope and phase-matching functions. As discussed above, the widths of these functions are related to the pump bandwidth and the crystal length. To eliminate frequency correlations, these two parameters should be chosen so as to satisfy Eq. (17). For a pump field centered at 800 nm having a full width at half maximum (FWHM) bandwidth of 15 nm , the BBO crystal should have a length of 2.6 mm . As shown in Fig. 3(b), these parameters yield a joint spectral intensity nearly circular in shape, being slightly elongated along one axis. Note, however, that the signal and idler frequencies are uncorrelated. For a given down-conversion event, that is, the range of frequencies expected for either photon is independent of the frequency detected for its sibling.

Of course, the requisite group-velocity mismatch may be obtained at other wavelengths, as well. In BBO it is possible to eliminate frequency correlations in a degenerate collinear configuration as long as the center wavelengths of the signal and idler are within the range $1.169 \mu\text{m} < \lambda < 1.949 \mu\text{m}$. Different crystal materials, with different dispersive properties, yield additional wavelengths at which the group-velocity mismatch may be attained. The ranges for several common materials [9] are shown in Table I. The joint spectra tend to be highly elliptical for wavelengths near the upper and lower limits of these ranges and become more circular near the center. They are exactly circular, in fact, at the wavelengths for which $k'_p - k'_s = k'_i - k'_p$. The wavelengths that satisfy this condition for the materials listed in Table I are shown in the column marked, “group-velocity matching.” When the group-velocity matching condition is satis-

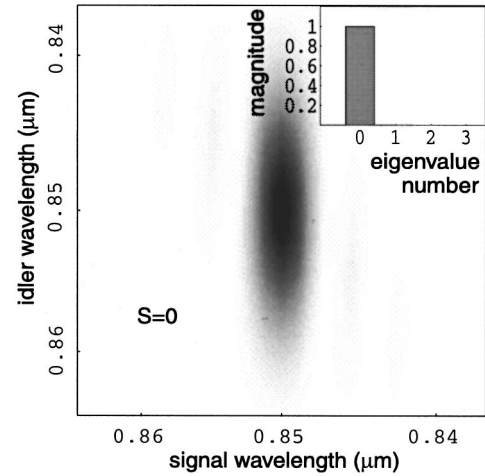


FIG. 4. The joint spectral intensity for degenerate type-II down-conversion in ADP with a 425 nm pump. The inset shows the details of the Schmidt decomposition.

fied, the signal and idler have identical spectra and the reciprocal group velocity of the pump is equal to the average of the signal and idler reciprocal group velocities. An interesting consequence in this case, as pointed out in [10], is that the signal and idler photons are indistinguishable (from each other) for all crystal lengths and pump bandwidths, except for an easily compensated difference in average emission times. This has important consequences in experiments involving only single pairs of frequency-degenerate photons, where the two-photon wave function is required to be symmetric but need not be free of correlations. We remind the reader, however, that in multisource experiments, the distinguishing information is carried in the correlations. Thus, the group-velocity condition alone is not sufficient for the elimination of unwanted spectral information—it is also necessary to choose the pump bandwidth and crystal length appropriately.

Of the crystals listed, ammonium dihydrogen phosphate (ADP) seems to be the best suited for incorporation into existing experimental schemes. Indeed, the lower limit corresponds to a pump wavelength of 411 nm , which is easily generated via second-harmonic generation of the output of a Ti:sapphire laser. Figure 4 shows the joint spectral intensity for an ADP crystal pumped by a field centered at 425 nm and having a FWHM bandwidth of 3 nm . It is clear from the figure that the signal and idler frequencies are uncorrelated. That is, the joint spectrum may be represented as the product of the individual spectra. The fact that the two spectra are markedly different does not introduce distinguishability into a multisource experiment as long as care is taken to ensure that the interference process does not involve the mixing of the signal from one crystal with the idler from another. Even though ADP seems to offer a means of eliminating frequency correlations, experimental implementation may be difficult. At the lower limit of the mismatch range, the crystal length required by Eq. (17) is quite large, having a value of $L = 4.8 \text{ mm}$ for the plot in Fig. 4. In this regime, it is likely that effects not considered in this treatment will be important.

The calculations carried out above show that it is possible

to eliminate frequency correlations for any down-conversion crystal in which the group velocity of the pump falls somewhere between the group velocities of the signal and idler. As demonstrated in the examples, however, experimental constraints such as wavelength accessibility may put this condition out of reach. It is possible, nonetheless, to choose the pump bandwidth and crystal length in such a way so as to minimize the frequency correlation in such cases. One method for quantifying the degree to which a two-photon wavefunction is factorable is to perform a Schmidt decomposition [11], which consists of finding a biorthogonal system $\{u_m(\omega)\}$, $\{v_m(\omega)\}$ such that $f(\omega_s, \omega_i)$ may be written as

$$f(\omega_s, \omega_i) = \sum_m \sqrt{\lambda_m} u_m(\bar{\omega}_s) v_m(\omega_i), \quad (18)$$

where λ_k , $u_k(\omega)$, and $v_k(\omega)$ satisfy the eigenvalue equations,

$$\begin{aligned} \int K_1(\omega, \omega') u_m(\omega') d\omega' &= \lambda_m u_m(\omega), \\ \int K_2(\omega, \omega') v_m(\omega') d\omega' &= \lambda_m v_m(\omega), \end{aligned} \quad (19)$$

with $K_1(\omega, \omega') = \iint f(\omega, \omega_2) f^*(\omega', \omega_2) d\omega_2$ and $K_2(\omega, \omega') = \iint f(\omega_1, \omega) f^*(\omega_1, \omega')$. The amount of spectral entanglement may be quantified by the degree of nonseparability of $f(\omega_s, \omega_i)$. One such measure is given by the entropy of entanglement,

$$S = - \sum_{k=0}^{\infty} \lambda_k \log_2 \lambda_k. \quad (20)$$

For the two-photon state having no frequency correlations, $f(\omega_s, \omega_i)$ is completely factorable and there is only a single nonzero term on the right-hand side of Eq. (18). The entropy of entanglement in this case is zero, i.e., there is no spectral entanglement. The more terms present on the right-hand side of Eq. (18) the greater the spectral entanglement as quantified by the entropy of entanglement, and also the higher the correlation between the signal and idler frequencies.

Depending on the specific form of the two-photon probability amplitude, calculation of the entropy may be quite difficult, often requiring numerical methods to solve the eigenvalue equations (19) [12]. For the special case in which the phase-matching and pump envelope functions may be described as in Eqs. (14) and (15), it is possible to carry out the Schmidt decomposition analytically. In this case, the eigenfunctions are the Hermite functions and the eigenvalues are

$$\lambda_n = \frac{\mu^{2n}}{\pi(1-\mu^2)}, \quad (21)$$

where $\mu = (1 - \sqrt{1 - \rho^2})/|\rho|$ and

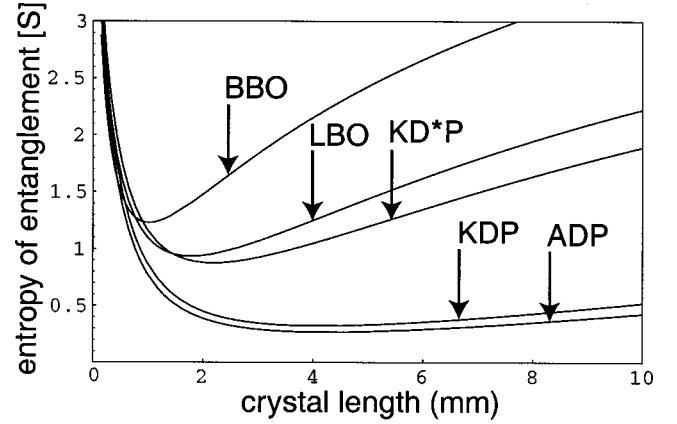


FIG. 5. The entropy of entanglement for several common crystal materials, plotted as a function of crystal length. The center pump wavelength was assumed to be 400 nm and the pump FWHM bandwidth was set to 3 nm.

$$\rho = - \frac{\frac{1}{\gamma\sigma^2} + L^2(k'_p - k'_s)(k'_p - k'_i)}{\sqrt{\left[\frac{1}{\gamma\sigma^2} + L^2(k'_p - k'_s)^2\right] \left[\frac{1}{\gamma\sigma^2} + L^2(k'_p - k'_i)^2\right]}}. \quad (22)$$

The parameter ρ is constrained to take values between -1 and 1 , and is zero when $f(\omega_s, \omega_i)$ is completely factorable. We stress that the analytic Schmidt decomposition presented here is valid only for type-II collinear down-conversion, in a regime where the Gaussian approximation [given in Eq. (11)] and the truncation of the phase mismatch at first order [again as given in Eq. (11)] are acceptable. In general, these approximations will be less adequate at large deviations from the central frequencies ω_{s0} and ω_{i0} . Examples of Schmidt decompositions calculated using the above equations are shown graphically in the insets of Figs. 1, 3, and 4. The entropy of entanglement is also shown for each case. Note the relationship between the shape of the joint spectrum and the corresponding Schmidt expansion. The more spectral correlation, i.e., the further the joint spectrum is from being aligned with the signal and idler axes, the greater the number of Schmidt modes having appreciable amplitudes, and also the higher the entropy of entanglement.

The dependence of the entropy of entanglement on crystal length is shown in Fig. 5 for several materials. For this plot, the center pump wavelength was assumed to be 400 nm and the pump FWHM bandwidth was set to 3 nm. Note that although the entropy of entanglement does not reach zero for any of the materials shown, it tends to be lower for ADP. Note also that with the pump field specified, there is an optimum crystal length for each crystal material. The crystal length for which the entropy of entanglement attains its smallest value is simply the length for which $|\rho|$ is minimized. For the case in which the group velocity of the pump is either greater than or less than the group velocities of the signal and idler photons, ρ cannot be made to vanish, but reaches its minimum in absolute value when the crystal length is

$$L = \frac{1}{\sigma} \sqrt{\frac{1}{\gamma(k'_p - k'_s)(k'_p - k'_i)}}. \quad (23)$$

When this crystal length is used, the frequency correlation is reduced, but not eliminated. Whether it is small enough depends, of course, on the particular experimental configuration.

The technique proposed in this paper suggests a different approach to the management of distinguishing information in experiments involving multiple pairs of photons. Instead of removing the unwanted information via some filtering process, the source is reconfigured so that the distinguishing information is never present. One way that this may be accomplished is to choose the parameters of the down-conversion source such that it produces pairs of photons that are uncorrelated in frequency and, consequently, in space time. Such sources are preferred because each photon carries no spectral or temporal information betraying its source or even the identity of its conjugate. Because no supplemental spectral filtering is required, the emission rate is likely to be

several orders of magnitude higher than for existing sources (by our estimates, the count rate cited in Ref. [3] would increase by a factor of greater than 10^4 if the spectral filters were not necessary). In cases in which it is not possible to attain the group-velocity mismatches needed to completely eliminate frequency correlations, it is still possible to choose parameters that will minimize these correlations.

ACKNOWLEDGMENTS

This research was supported by an award from Research Corporation and was partially supported by the Engineering Research Program of the U.S. Department of Energy, Office of Basic Energy Sciences under Contract No. DE-AC05-00OR22725 with UT-Battelle, LLC. It was also supported by the National Science Foundation and the Center for Quantum Information, and by the Army Research Office through the MURI program (DAAD 19-99-1-0215). We thank Konrad Banaszek for the original idea of analytic Schmidt decomposition using a Gaussian approximation of the phase-matching function [13].

-
- [1] D. Bouwmeester *et al.*, Nature (London) **390**, 575 (1997); D. Bouwmeester *et al.*, Appl. Phys. B: Lasers Opt. **67**, 749 (1998).
- [2] J. Pan *et al.*, Phys. Rev. Lett. **80**, 3891 (1998).
- [3] D. Bouwmeester *et al.*, Phys. Rev. Lett. **82**, 1345 (1999).
- [4] J. Pan *et al.*, Nature (London) **403**, 515 (2000).
- [5] B. Yurke and D. Stoler, Phys. Rev. Lett. **68**, 1251 (1992).
- [6] A. Zeilinger *et al.*, Phys. Rev. Lett. **78**, 3031 (1997).
- [7] M. Zukowski *et al.*, Phys. Rev. Lett. **71**, 4287 (1993).
- [8] W. Grice and I. Walmsley, Phys. Rev. A **56**, 1627 (1997).
- [9] V. G. Dmitriev, G. G. Gurzadyan, and D. N. Nikogosyan, *Handbook of Nonlinear Optical Crystals* (Springer-Verlag, Berlin, 1991).
- [10] T. E. Keller and M. H. Rubin, Phys. Rev. A **56**, 1534 (1997).
- [11] S. Parker, S. Bose, and M. B. Plenio, Phys. Rev. A **61**, 032305 (2000).
- [12] C. K. Law, I. A. Walmsley, and J. H. Eberly, Phys. Rev. Lett. **84**, 5304 (2000).
- [13] K. Banaszek and J. H. Eberly (unpublished).